Effect of noise and inertia on modulation-induced negative differential resistance

L. N. Gwaki, C. J. Lambert, R. Mannella,* and P. V. E. McClintock

School of Physics and Materials, Lancaster University, Lancaster LA1 4YB, United Kingdom

(Received 18 November 1992)

It is demonstrated that modulation-induced negative differential resistance can survive in the presence of noise and inertia. In the limit of large periodic forcing, by perturbing about the overdamped, noise-free system, analytic predictions for the effects of weak noise or small inertia are obtained. These are shown to compare well with the results of detailed numerical simulations.

I. INTRODUCTION

During the past two decades, the transition to chaos of deterministic, nonlinear systems has received a great deal of attention. In contrast, prechaotic transitions in deterministic and stochastic systems have been much less intensively studied. Examples of the latter are noise-induced transitions of the type found in low-order evolution equations.[1-6] Another example, which is the focus of interest in the present paper, is the onset of modulation-induced negative differential resistance (MINDR), where the response of a periodically driven system decreases with increasing drive amplitude.[7,8] For an overdamped system, in the limit of very slow changes, this phenomenon is to some extent trivial, since parametric changes can cause the system to jump from one equilibrium position of the instantaneous potential to another. The situation in the limit of high-frequency forcing is less straightforward and until now only the noise-free, overdamped case has been studied.[7,8] Since the neglect of inertia and noise is often an idealization of a real situation, there is a need for a description which includes these effects and which demonstrates that MINDR survives in their presence. The aim of the present paper is to provide such a description.

In Ref. 8, as a paradigm of MINDR, the inertia and noise-free equation

$$dx/dt = f(x) + V_0 h(t)g(x) \tag{1.1}$$

was studied, where the periodic modulation $h(t)$, of period τ, satisfies

$$\int_0^\tau dt\, h(t) = 0, \quad \tau^{-1}\int_0^\tau dt\, |h(t)| = 1,$$

and V_0 is the amplitude of forcing. After transients have receded, the response $x(t)$ varies periodically between two limits x_+, x_-, whose value, in the presence of a square wave modulation, can be determined by solving a pair of simultaneous nonlinear equations, obtained after dividing Eq. (1.1) by the quantity $V_0 h(t)g(x)$ and integrating over each half cycle. In the high-frequency, large forcing regime defined by $\tau \to 0$, $V_0 \to \infty$, with $\mu = V_0\tau/2 = $ finite, the sum and difference of this pair of autonomous equations, reduce to the simple form

$$\int_{x_-}^{x_+} dx\, f(x)/g^2(x) = 0, \tag{1.2}$$

$$\int_{x_-}^{x_+} dx\, g^{-1}(x) = \mu. \tag{1.3}$$

After evaluating the integrals, one is left with two simultaneous equations for the unknown quantities $x_\pm$.

Equations (1.2) and (1.3) demonstrate that in the large-V_0 limit, the response amplitude $|x_+ - x_-|$ depends only on the impulse parameter μ and not on the separate quantities V_0, τ. Consequently, keeping V_0 fixed and varying τ yields the same result as keeping τ fixed and varying V_0. This is in marked contrast with a harmonic oscillator, where the response is simply scaled by V_0. More important, it was also shown in Ref. 8 that if $h(t)$ is an arbitrary waveform, whose deviation from a square wave is characterized by a coefficient of castellation ϵ, then the above equations remain valid, provided f is replaced by the modified function

$$\tilde{f}(x,\epsilon) = f(x) - \epsilon g(x). \tag{1.4}$$

This is a useful result, since it reveals that if in the presence of square wave forcing, the limits $x_+(\mu,\epsilon)$ and $x_-(\mu,\epsilon)$ of the modified equation

$$dx/dt = \tilde{f}(x,\epsilon) + V_0 h(t)g(x) \tag{1.5}$$

are known, then they are known for all other periodic forms of $h(t)$. In what follows, it will be shown that in the limit of weak noise and/or small inertia, the response can also be obtained from the solution of an equation of the form (1.5).

II. THE EFFECT OF INERTIA ON MINDR

In the presence of a nonzero mass m, Eq. (1.1) generalizes to

$$m\,d^2x/dt^2 + dx/dt = f(x) + V_0 h(t)g(x). \tag{2.1}$$

In Ref. 8, as a specific example, the following choice of $f(x)$ and $g(x)$ was made:

$$f(x) = -x^3 + \lambda_0 x^2 - Qx + R \tag{2.2}$$

and

$$g(x) = x^2 \qquad (2.3)$$

with $\lambda_0 = 3.6$, $Q = 3$, and $R = 0.7$. These values were chosen to yield three real roots for $f(x)$. To illustrate the effect of inertia, we first adopt this particular choice for f and g and show the results of a digital simulation of Eq. (2.1). For convenience, we define $x_+ > x_-$ and, following Ref. 8, show results only for x_+. For large V_0, provided results are plotted against the impulse parameter μ, fixing τ and varying V_0 yields the same response as fixing V_0 and varying τ. With $V_0 = 10$ and varying τ, Fig. 1 shows how curves of x_+ versus μ change with increasing m. These demonstrate that the regions of negative slope, which are a signature of MINDR, not only survive in the presence of inertia, but for this choice of parameters are initially enhanced as m increases from zero.

For finite m, Eq. (2.1) can, of course, undergo a period doubling transition, such that x_+ and MINDR are no longer defined. Since we are interested primarily in describing MINDR, we restrict the analysis to small m and develop a perturbative result for x_+. To this end it is convenient to rearrange Eq. (2.1) in the form

$$dx/dt = f(x) + g(x)V_0 h(t) - m d^2 x/dt^2 . \qquad (2.4)$$

Differentiating this equation with respect to time and substituting the result back into (2.4) yields, after retaining terms which are at most linear in m,

$$dx/dt = f(x) + g(x)[V_0 h(t) - mV_0 dh(t)/dt]$$
$$- m[df/dx + V_0 h(t)dg/dx]$$
$$\times [f(x) + g(x)V_0 h(t)] . \qquad (2.5)$$

To isolate the leading term when $g(x)$ is not a constant, it is convenient to define the parameter $\beta = mV_0^2$, such that when $m \to 0$, and $V_0 \to \infty$, β is finite. In this limit, $\beta/V_0 = mV_0$ is negligible compared with mV_0^2 and Eq. (2.5) reduces to
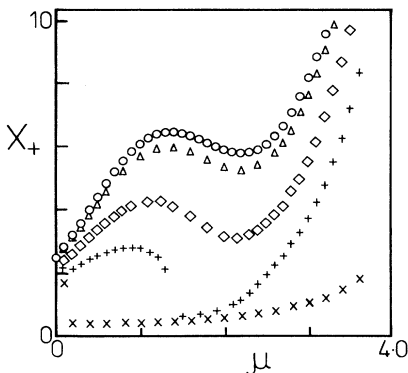

FIG. 1. Numerical results for x_+ v μ obtained with fixed $V_0 = 10$ and various values of the mass m. Since for large V_0, an identical response is obtained for fixed τ and varying V_0, the regions of negative slope indicate the presence of MINDR. The $\bigcirc$ corresponds to $m = 10^{-5}$, the $\triangle$ to $m = 10^{-4}$, the $\Diamond$ to $m = 5 \times 10^{-4}$, the $+$ to $m = 10^{-3}$, and the $\times$ to $m = 5 \times 10^{-3}$. Adopting the convention of Ref. 8, we identify MINDR with the existence of regions of negative slope.

$$dx/dt = F(x) + g(x)V_0 h(t) , \qquad (2.6)$$

where

$$F(x) = f(x) - \beta g(x)dg(x)/dx . \qquad (2.7)$$

Hence the system with small inertia has been mapped onto an overdamped system, but with a modified $f(x)$. For the simple cubic of Eq. (1.2),

$$F(x) = -(1 + 2\beta)x^3 + \lambda_0 x^2 - Qx + R .$$

The analysis of Ref. 8 can now be used to obtain results for x_+ in the small mass limit. An example of these results is shown in Fig. 2 for different values of β, while in Fig. 3, a comparison with numerical results is shown. Shown also in Fig. 4 is a comparison between analytical and numerical results when $g(x) = x$. In both cases, for small m, good agreement is obtained.

The analysis of Ref. 8 shows that in the impulse limit, an overdamped system cannot exhibit MINDR unless it is multistable in the absence of forcing. Since (2.6) and (2.7) map the system with inertia onto an equivalent overdamped problem, the former will only exhibit MINDR if $F(x)$ has more than one root. In moving from $\beta = 0.1$ to 0.5, the number of roots changes from 3 to 1, so MINDR disappears. More generally, the range of β for which $F(x)$ possesses more than one root will depend on the precise form of $f(x)$ and $g(x)$. This range may therefore increase or decrease upon changing $g(x)$ from x to x^2.

The results (2.6) and (2.7) can be applied to a wide range of functions $f(x)$ and $g(x)$, provided that $g'(x) \neq 0$. If this is not the case, the lowest-order correction is lost when taking the limit $\beta/V_0 \to 0$. To obtain a perturbative result when $g(x)$ is a constant, we return to (2.7) and note that if $h(t)$ is a square wave then its derivative is of the form

$$dh(t)/dt = \sum_{n=0}^{\infty} \{ -\delta[t - (n + \tfrac{1}{2})\tau] + \delta(t - n\tau) \} .$$

Consequently, after integrating Eq. (2.5), we obtain discontinuities in $x(t)$ at $t = (n + \tfrac{1}{2})\tau$ and $t = n\tau$ of magnitude mV_0. Hence with $g(x) = 1$, integrating over the half cycle for which $h(t) = 1$, yields
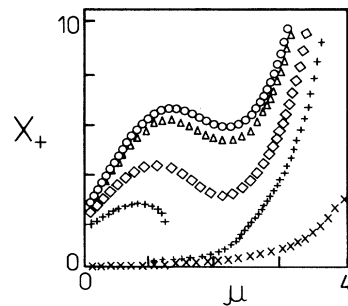

FIG. 2. Analytic results for x_+ vs μ, obtained by solving Eq. (1.2) and (1.3) after first replacing $f(x)$ by $F(x)$, defined in (2.7). For fixed $V_0 = 10$, results are shown for various values of the mass m: the $\bigcirc$ corresponds to $\beta = 10^{-3}$, the $\triangle$ to $\beta = 10^{-2}$, the $\Diamond$ to $\beta = 5 \times 10^{-2}$, the $+$ to $\beta = 0.10$, and the $\times$ to $\beta = 0.50$.
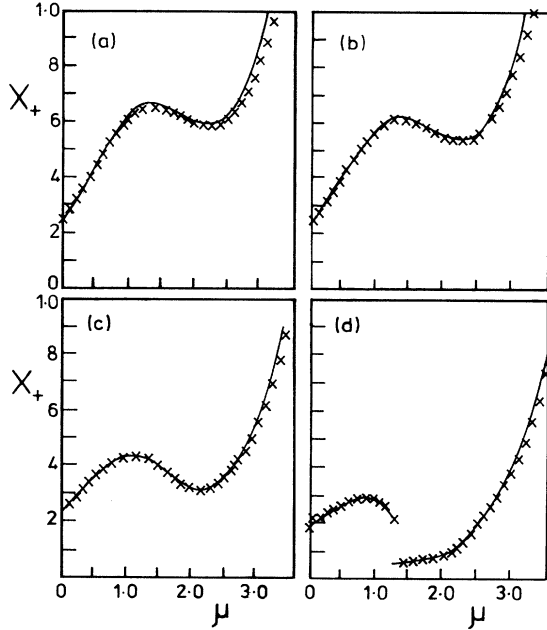
FIG. 3. A comparison of theoretical (solid line) and numerical ($\times$) results when $g(x)=x^2$, for the following parameter values: (a) $\beta=10^{-3}$, (b) $\beta=0.01$, (c) $\beta=0.05$, and (d) $\beta=0.1$. In all cases $V_0=10$.

$$\int_{x_-}^{x_+ - mV_0} \frac{dx}{F_1(x)+V_0} = \tau/2 \ ,$$

where

$$F_1(x) = f(x) - m\frac{df}{dx}[f(x)+V_0] \ .$$

Similarly, for the half cycle $h(t)=-1$,

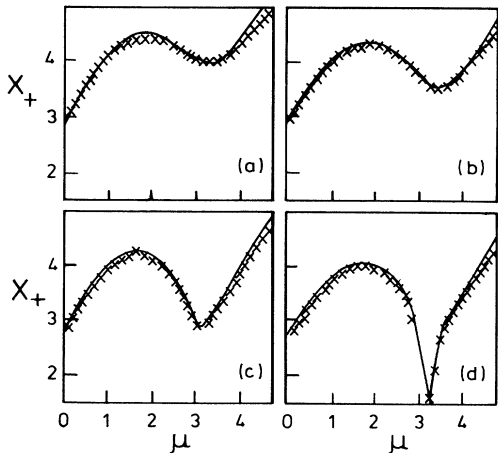$$\int_{x_+}^{x_- + mV_0} \frac{dx}{F_2(x)-V_0} = \tau/2 \ ,$$

FIG. 4. A comparison between theoretical (solid line) and numerical ($\times$) results when $g(x)=x$, $V_0=10$, and (a) $\beta=0.01$, (b) $\beta=0.10$, (c) $\beta=0.15$, and (d) $\beta=0.18$.
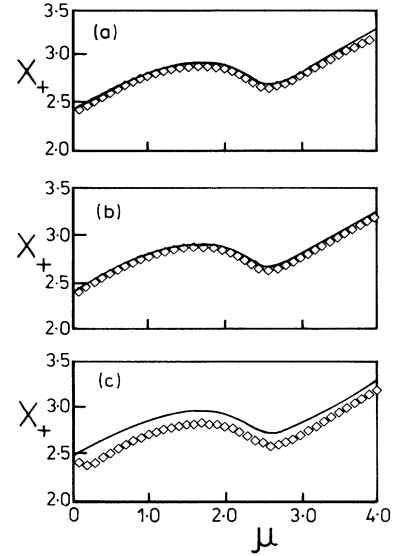

FIG. 5. A comparison between theoretical (solid line) and numerical ($\diamond$) results, when $g(x)=1$, $V_0=10$, and (a) $\alpha=10^{-3}$, (b) $\alpha=10^{-2}$, and (c) $\alpha=0.1$.

where

$$F_2(x) = f(x) - m\frac{df}{dx}[f(x)-V_0] \ .$$

To lowest order in mV_0, these equations can be written as

$$\int_{x_-}^{x_+} \frac{dx}{F_1(x)+V_0} - \frac{mV_0}{F_1(x_+)+V_0} = \tau/2$$

and

$$\int_{x_-}^{x_+} \frac{dx}{F_2(x)-V_0} - \frac{mV_0}{F_2(x_-)-V_0} = -\tau/2 \ ,$$

respectively. In the limit $m\to 0$, $V_0\to\infty$, but $\alpha=mV_0$ finite, these can be combined to yield

$$\int_{x_-}^{x_+} f(x)dx - \alpha/2[f(x_+)+f(x_-)] = 0 \qquad (2.8)$$

and

$$\int_{x_-}^{x_+} dx = \mu + \alpha \ . \qquad (2.9)$$

Again one obtains simultaneous equations for $x_\pm$. A comparison between the solution of this pair of equations and the results of a numerical simulation is shown in Fig. 5.

III. THE EFFECT OF NOISE ON MINDR

The above analysis demonstrates not only that MINDR survives in the presence of inertia, but also that for small m and large V_0 the changes which occur can be conveniently described by perturbing about the overdamped limit. In this section, we examine the effect of

noise on MINDR with large forcing and again demonstrate that the overdamped system provides a useful starting point for a perturbative description.

The equation of interest is the (Stratonovich) stochastic differential equation,

$$dx/dt = f(x) + g(x)V_0 h(t) + g(x)\Gamma(t) ,\qquad (3.1)$$

where $\Gamma(t)$ is Gaussian white noise, satisfying $\langle \Gamma(t)\rangle = 0$ and $\langle \Gamma(t)\Gamma(t')\rangle = 2D\delta(t-t')$.

To demonstrate that MINDR survives when $D\neq 0$, we begin by showing the results of a numerical simulation of Eq. (3.1), carried out using the algorithm of Ref. 9, which employs the Stratonovich prescription for stochastic integrals. All numerical results were obtained in the large-V_0 limit, using the choice of functions (2.2) and (2.3). Since $x(t)$ is a random walk, the values $x_+^i = x(i\tau)$ and $x_-^i = x(i\tau - \tau/2)$, which arise at the switching times of a square wave modulation $h(t)$, are now random variables. After transients have disappeared, the quantities of interest are the distributions or equivalently the moments of these variables. An example of the former is given in Fig. 6, which for $D = 0.01$ shows the variation of the distributions of x_+ with μ. This demonstrates that in a probabilistic sense, MINDR persists in the presence of noise. Figure 6 is typical of the behavior we have observed for a range of parameter values and shows that as $D \to 0$, the
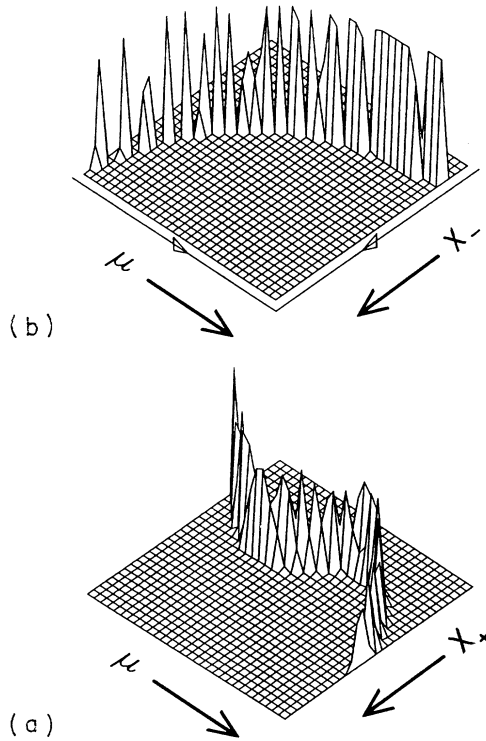

FIG. 7. Numerical results for $\langle x_+(\mu)\rangle$ obtained for various noise strengths: $D = 0.01$ ($\bigcirc$); $D = 0.1(\times)$; $D = 0.2(+)$; $D = 0.3$ ($\square$).

distributions approach δ functions centered on the noise-free values $\bar{x}_x, \bar{x}_-$. As D increases, the distributions broaden and the peak positions shift. To illustrate this behavior, we focus attention on the mean and standard deviations of these distributions. A selection of numerical results for $\langle x_+(\mu)\rangle$ is shown in Fig. 7, which demonstrates that, with increasing noise, the regions of negative slope of $\langle x_+(\mu)\rangle$ are shifted. The aim now is to develop a perturbative result which quantifies this behavior.

To obtain an analytical solution in the limit of large forcing, we divide Eq. (3.1) by $f(x) + g(x)V_0 h(t)$, integrate over each half cycle, and take the limit $V_0 \to \infty$. Writing

$$F_\pm(x) = [V_0 g(x) \pm f(x)]^{-1}\qquad (3.2)$$

yields

$$\int_{x_-^i}^{x_+^{i+1}} F_+(dx) = \frac{\tau}{2}\left[1 + \mu^{-1}\int_{i\tau}^{(i+1/2)\tau}\Gamma(t)dt\right] + O(\tau^{5/2})$$

$$(3.3)$$

and

$$\int_{x_-^{i+1}}^{x_+^{i+1}} F_-(x)dx = \frac{\tau}{2}\left[1 - \mu^{-1}\int_{(i+1/2)\tau}^{(i+1)\tau}\Gamma(t)dt\right] + O(\tau^{5/2}) ,$$

$$(3.4)$$

where the symbol $O(\tau^{5/2})$ on the right-hand sides, represents terms which vanish as $\tau^{5/2}$ in the impulse limit.

To obtain a perturbative result, Eq. (3.3) and (3.4) will now be expanded about the noise-free values $\bar{x}_\pm$, given by

(b)

(a)

FIG. 6. (a) and (b) show the probability distributions of x_+ and x_-, respectively, for $D = 0.01$. Before switching on the noise, the system was allowed to settle down, then for each value of μ, a distribution was formed from typically of order 10^5 subsequent values of $x_\pm$.
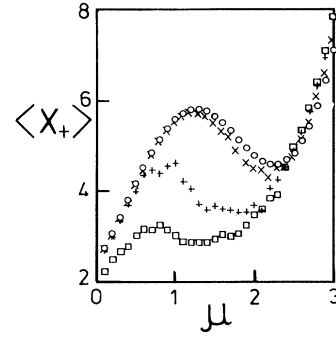
$$\int_{\bar{x}_-}^{\bar{x}_+} dx\, F_+(x) = \int_{\bar{x}_-}^{\bar{x}_+} dx\, F_-(x) = \frac{\tau}{2} .\qquad (3.5)$$

Writing $F_{\alpha\beta} = F_\alpha(x_\beta)$ yields, to second order,

$$F_{++}(x_+^{i+1}-\overline{x}_+)-F_{+-}(x_-^i-\overline{x}_-)+\tfrac{1}{2}F'_{++}(x_+^{i+1}-\overline{x}_+)^2-\tfrac{1}{2}F'_{+-}(x_-^i-\overline{x}_-)^2=\frac{\tau}{2\mu}\int_{i\tau}^{(i+1/2)\tau}\Gamma(t)dt+O(\tau^{5/2})$$

(3.6)

and

$$F_{-+}(x_+^{i+1}-\overline{x}_+)-F_{--}(x_-^{i+1}-\overline{x}_-)+\tfrac{1}{2}F'_{-+}(x_+^{i+1}-\overline{x}_+)^2-\tfrac{1}{2}F'_{--}(x_-^{i+1}-\overline{x}_-)^2=\frac{\tau}{2\mu}\int_{(i+1/2)\tau}^{(i+1)\tau}\Gamma(t)dt+O(\tau^{5/2}),$$

(3.7)

where $F'_{\alpha\beta}=\partial_{x_\beta}F_\alpha(x_\beta)$.

Starting from these equations, it is straightforward to develop a hierarchy of coupled moment equations. For example, averaging Eqs. (3.6) and (3.7) yields

$$F_{++}a_+-F_{+-}a_-+\tfrac{1}{2}F'_{++}\sigma_+-\tfrac{1}{2}F'_{+-}\sigma_-=O(\tau^{5/2})$$

(3.8)

$$F_{-+}a_+-F_{--}a_-+\tfrac{1}{2}F'_{-+}\sigma_+-\tfrac{1}{2}F'_{--}\sigma_-=O(\tau^{5/2}),$$

(3.9)

where $a_\pm=\langle x_\pm-\overline{x}_\pm\rangle$ and $\sigma_\pm=\langle(x_\pm-\overline{x}_\pm)^2\rangle$.

To first order in V_0^{-1}, the left-hand sides of these equations are not linearly independent and therefore for large V_0 it is necessary to retain terms up to order V_0^{-2}. Despite this feature, the $O(\tau^{5/2})$ terms on the right-hand sides do not contribute in the impulse limit and will therefore be ignored. Consequently if $\sigma_\pm$ are known, then $a_\pm$ are determined and vice versa.

To obtain further moment equations, one could, for example, square and average Eqs. (3.6) and (3.7). However, even after retaining only second-order terms, this does not lead to a closed set of equations because higher-order correlations are introduced. To obtain a second pair of equations, we instead rearrange (3.6) and (3.7) to eliminate $(x_-^i-\overline{x}_0)$ from the left-hand side of Eq. (3.6) and $(x_+^{i+1}-\overline{x}_+)$ from (3.7). This yields

$$(x_+^{i+1}-\overline{x}_+)=\theta(x_+^i-\overline{x}_+)+\eta_i+\text{squared terms}$$

(3.10)

and

$$(x_-^{i+1}-\overline{x}_-)=\theta(x_-^i-\overline{x}_-)+\chi_i+\text{squared terms},$$

(3.11)

where

$$\theta=\frac{F_{+-}F_{-+}}{F_{++}F_{--}},$$

$$\eta_i=\frac{\tau}{2\mu F_{++}}\left[\int_{i\tau}^{(i+1/2)\tau}\Gamma(t)dt+\frac{F_{+-}}{F_{--}}\int_{(i-1/2)\tau}^{i\tau}\Gamma(t)dt\right],$$

and

$$\chi_i=\frac{\tau}{2\mu F_{--}}\left[\int_{(i+1/2)\tau}^{(i+1)\tau}\Gamma(t)dt+\frac{F_{-+}}{F_{++}}\int_{i\tau}^{(i-1/2)\tau}\Gamma(t)dt\right].$$

Equations (3.10) and (3.11) can now be solved by iteration. For example, if θ is less than unity, Eq. (3.10) can be iterated to yield

$$(x_+^{i+1}-\overline{x}_+)=\theta^{n+1}(x_+^{i-n}-\overline{x}_+)$$
$$+\sum_{j=0}^n\theta^j\eta_{i-j}+\text{squared terms}.\quad(3.12)$$

For $\theta<1$, as $n\to\infty$, the first term on the right-hand side vanishes. Since $\langle\eta_i\eta_j\rangle=\delta_{ij}\phi_+$ and $\langle\chi_i\chi_j\rangle=\delta_{ij}\phi_-$, where for large V_0 the leading contribution to $\phi_\pm$ is given by

$$\lim_{V_0\to\infty}\phi_\pm\to2\tau Dg^2(\overline{x}_\pm),$$

squaring and averaging Eq. (3.12) yields, to lowest order,

$$\sigma_+=\phi_+\sum_{j=0}^\infty\theta^{2j}=\phi_+/(1-\theta^2).$$

For $\theta>1$, the equation obtained by dividing (3.10) by θ can be iterated to yield $\sigma_+=\phi_+/(\theta^2-1)$. After applying the same procedure to Eq. (3.11), one obtains the combined result

$$\sigma_\pm=\phi_\pm/(|1-\theta^2|),$$

which, in the limit $V_0\to\infty$, simplifies to

$$\sigma_\pm=\frac{\mu Dg^2(\overline{x}_\pm)}{[|f(\overline{x}_+)/g(\overline{x}_+)-f(\overline{x}_-)/g(\overline{x}_-)|]}.\quad(3.13)$$

Finally, substituting this into Eqs. (3.8) and (3.9) yields, for the mean values,

$$a_\pm=\pm\frac{sD\mu g_\pm}{2\left[\dfrac{f_-}{g_-}-\dfrac{f_+}{g_+}\right]^2}[f'_\pm-f'_\mp+(g'_++g'_-)f_\mp/g_\mp$$
$$-2f_\pm g'_\pm/g_\pm],\quad(3.14)$$

where $s=$ sign of $(f_-/g_--f_+/g_+)$.

A comparison with numerical results for $\langle x_+\rangle=\overline{x}_++a_+$ and $\sigma_+^{1/2}$ is shown in Fig. 8. Again, for small D, good agreement is obtained.
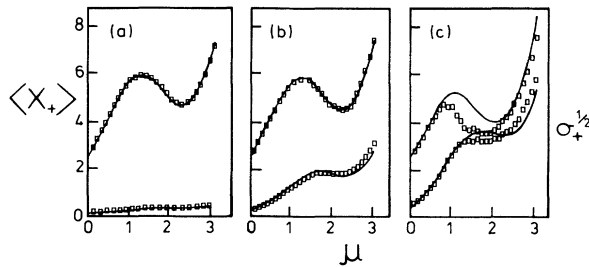
FIG. 8. Numerical ($\square$) and perturbative (solid lines) results for $\langle x_+ \rangle$ vs μ (upper curves) and $\sigma_+^{1/2}$ vs μ (lower curves) for (a) $D=0.01$, (b) $D=0.1$, and (c) $D=0.2$.

IV. DISCUSSION

The aim of this paper has been to demonstrate that MINDR survives in the presence of noise and inertia and to show that, in the impulse limit, the overdamped, noise-free system provides a useful starting point for a perturbative description of their effects. In Sec. II, it was shown that for multiplicative forcing, the leading contri-

bution can be obtained from an overdamped system, with a modified force given by Eq. (2.7). The extra term on the right-hand side of this equation is reminiscent of corrections due to noise-induced drift in stochastic differential equations subject to multiplicative white noise,[3] which arise when different versions of stochastic calculus are used. When the forcing is additive, this correction vanishes and the leading term is then obtained from the generalizations (2.8) and (2.9) of the inertia-free equations (1.2) and (1.3).

In Sec. III, the effect of white noise is examined. Again in the impulse limit, the effect of weak noise is described by perturbing about the noise-free solutions $\bar{x}_+$. A novel feature of these results is that the sign of $da_+/d\mu$ can be changed by varying the noise strength D. For this reason, MINDR in the presence of noise provides a new example of a noise-induced transition in nonlinear systems.

*Now at Dipartimento di Fisica, Università degli Studi di Pisa, Piazza Torricelli 2, 56100 Pisa, Italy.
[1]S. R. Landauer, J. Appl. Phys. 33, 2209 (1962).
[2]G. V. Welland and F. Moss, Phys. Lett. 89A, 273 (1982).
[3]W. Horsthemke and R. Lefever, Noise Induced Transitions: Theory and Applications in Physics, Chemistry and Biology (Springer-Verlag, Berlin, 1984).
[4]K. Lindenberg and B. West, Physica A 128, 25 (1984).
[5]A. Hernandez-Machado, M. San Miguel, and J. M. Sancho, Phys. Rev. A 9, 3388 (1984).
[6]W. Horsthemke, C. R. Doering, R. Lefever, and A. S. Chi,

Phys. Rev. A 31, 1123 (1985).
[7]R. C. M. Dow, C. J. Lambert, R. Mannella, P. V. E. McClintock, and F. E. Moss, in Noise in Physical Systems and 1/f Noise, edited by A. D'Amico and P. Mazzetti (Elsevier, Amsterdam, 1986), p. 133.
[8]R. C. M. Dow, C. J. Lambert, R. Mannella, and P. V. E. McClintock, Phys. Rev. Lett. 59, 6 (1987).
[9]R. Mannella, in Noise in Non-linear Dynamical Systems, edited by F. Moss and P. V. E. McClintock (Cambridge University Press, Cambridge, 1989), Vol. III, p. 189.